A Novel Approach to Denoising Impulse Noise in Satellite Images Using Adaptive Switching Trimmed Vector Median Filter

Y.Vishnu Tej[1], M. James Stephen[2], P.V.G.D. Prasad Reddy[3]

[1]Research Scholar, Department of Computer Science and Systems Engineering, Andhra University, Visakhapatnam, AP, INDIA.

[2]Professor, Department of Computer Science and Engineering, WISTM Engineering College, Visakhapatnam, AP, INDIA.

[3]Professor, Department of Computer Science and Systems Engineering, Andhra University, Visakhapatnam, AP, INDIA.

Corresponding Author email: [1]vishnutej.br@gmail.com

Article Info
Page Number: 5640-5653
Publication Issue:
Vol. 71 No. 4 (2022)

Article History
Article Received: 25 March 2022
Revised: 30 April 2022
Accepted: 15 June 2022
Publication: 19 August 2022

Abstract

In this paper, a novel filtering approach was presented to remove the impulse noise in satellite images. Generally, satellite images are affected by speckle, Gaussian, and impulse noise. It is essential to remove the noise present in the image by applying appropriate filters. By attenuating the high-frequency image components and removing noise from the image, essential features are also lost. Due to their exhaustive search mechanism, the widely used median filter and its variants and switching filter methods, which demonstrate good noise reduction, suffer greatly from computational complexity. With these methods, each pixel in a test window is compared against every other pixel to reach a consensus on the accuracy of the test pixel. This paper presents a novel filtering method for denoising satellite images using the Adaptive Switching Trimmed Vector Median Filtering approach, and it has given better performance when compared to the existing algorithms in terms of peak signal-to-noise ratio (PSNR), structure similarity index (SSIM), and root means square error (RMSE).

Keywords: Impulse Noise, Median Filter, Vector Median Filter, Image Denoising, Adaptive Switching trimmed VMF.

Introduction

Noise is a common cause of satellite image corruption during capture and transmission. Image denoising is used to reduce the amount of noise while preserving the key signal characteristics. Image denoising algorithms are required to stop this kind of digital image degradation [1]. Numerous environmental applications, such as the control of weather, floods, and fires, as well as the tracking of earth resources and geographic mapping, agricultural crop forecasting, and urban growth, all benefit from the use of satellite images. The space imaging application includes the identification and evaluation of objects in images obtained from deep space probe missions [2]. When salt and pepper noise is added to satellite images, it typically results from a noisy image threshold and has sporadic occurrences of both black and white intensity values. On satellite images, the noise, which appears as black and white dots, significantly reduces the visual impact of the image.

Using the well-known median filter and its modifications is one efficient way to get rid of impulsive noise [3][4][5]. Due to their much-increased filtering effectiveness in terms of edge/detail retention and impulse noise attenuation, nonlinear filters have been extensively used. Traditional median filtering methods unconditionally perform the median operation to every pixel, regardless of whether it is uncorrupted or corrupted [6]. As a result, the uncorrupted pixels' contributions to the image details are still vulnerable to filtering, which reduces the quality of the image.

To characterize the grey or color difference between pixels and their neighbouring pixels at various sizes, a multilayer weighted graph model is developed. The graph node with the lowest strength is then found via a transformation of the noise detection [13]. The neighbourhood pixel values are sorted into numerical order to get the median, which is then used to replace the pixel in the issue. The average of the two middle pixel values is used when the neighbourhood has an even number of pixels [14].

To minimize multichannel dependence, color and satellite images are processed using a nonlinear method called the vector median filter (VMF). The filters in this family, especially the VMF, may perform rather well in impulse noise reduction without producing color distortions because they appropriately handle the color component correlation [15][16]. By substituting another pixel in the window for the test pixel in this method, the total distance between all pixels is decreased.

Based on the direction of the image vectors, the VDF (vector directional filter) divides the processing of image data into "directional processing" and "magnitude processing." Processing of image data that solely takes into account, directional information in the vector space is referred to as "directional processing." Magnitude processing, on the other hand, applies to image data processing that only takes vector magnitudes into account. Vector signal processing and single-channel image processing are connected by the VDF's separation of the processing feature [17].

The basic vector directional filter (BVDF) suggests utilizing direction instead of distance as a substitute. By employing the angular distance between pixels rather than vector magnitudes, this filter minimizes the aggregate angular distance over all pixels in the window [16][18]. Another image filtering technique is directional distance filtering (DDF), which employs a weighted product of VMF and BVDF [19].

The directional VMF (DVMF), which applies vector median filtering to pixels that are within a certain angle of the center test pixel, is another directed technique [20]. It has been demonstrated that the adaptive switching trimmed (AST) and adaptive rank-weighted switching (ARWSF) filters are efficient in reducing impulsive noise [20][21].

The so-called switching median filters [7]–[12] have demonstrated a considerable performance increase by including noise detection techniques or "intelligence" into the median filtering architecture. Early switching median filters have frequently been shown to be nonadaptive to a given, but unknown, noise density and prone to producing misclassified pixels, especially at greater noise level interference [12]. The adaptive switching trimmed vector median filtering algorithm described in this research is a unique method for denoising impulse noise in satellite images.

Adaptive Switching Trimmed Vector Median Filtering

The majority of filtering methods use n samples from a sliding, operational window W with the $x_{u,v}$ at its center to calculate the output for the pixel at position (u, v). The central pixel of W will be designated as x_1 to further simplify the analysis, and the other pixels will be marked as $x_1 \dots \dots x_n$ as shown in Fig. 1.

x_2	x_3	x_4
x_5	$x_{u,v}$ x_1	x_6
x_7	x_8	x_9

Fig.1 Notation of pixels in the filtering window

The reduced ordering technique is based on the sum of the distances (dissimilarity measures), indicated as d, between a particular pixel and the samples from the filtering window W, the cumulative dissimilarity measure D given to pixel xi, (i=1...n) from W, is

$$D_i = \sum_{j=1}^{n} d(x_i, x_j) \tag{1}$$

The distances $d_{ij} = d(x_i, x_j)$ between x_i and every other pixel x_j belonging to W, $(i, j = 1 \dots n, i \neq j)$, can be arranged in ascending order as follows:

$$d_{i1}, \dots, d_{iv} \rightarrow d_{i(1)}, \dots, d_{i(v)} \tag{2}$$

Where $v = n - 1$, Moreover, a trimmed sum of distances $\widehat{D}$ can be utilized in place of the aggregated distances in (1) [22].

$$\widehat{D}_i = \sum_{r=1}^{m} d_{i(r)} \tag{3}$$

where m represents the number of nearest pixels used in the trimmed sum of distances calculation and $d_{i(r)}$ represents the r^{th} least dissimilarity value. Compared to the usual sum of distances D_i, the trimmed sum $\widehat{D_i}$ is much more resistant to outliers among pixels of W [23][24].

One method of measuring pixel corruption is to use the value of $\widehat{D_1}$, which is given to the centre pixel x_1. When there are at least m identical pixels in the surrounding area, this number is low; otherwise, the centre pixel x_1 can be regarded as corrupted. If $\widehat{D_1}$ divided by m exceeds a predetermined threshold value, then T

$$\frac{\widehat{D_1}}{m} > T, \tag{4}$$

If W's center pixel is determined to be noisy, it will be replaced with the result of an appropriate robust filter; if not, it will be considered uncorrupted and will remain as is. In (4), the T value is made independent of the number of nearby pixels used to calculate $\widehat{D}$ by dividing by m. The decision-making process described above will be referred to as Switching Trimmed (ST).

Additionally, the noise array M's map is updated for each processed pixel,

$$M_{u,v} = \begin{cases} 0 & : \quad if\ recognised\ as\ corrupted \\ 1 & : \quad otherwise \end{cases} \tag{5}$$

This map will be used subsequently to replace the noisy pixels. Now, a kind of adaptability may be added to the ST scheme in order to address the impact of large values of the trimmed sum of distances $\widehat{D}$ in textured regions. This is done by subtraction the minimum value $\widehat{D_{(1)}}$ determined for the pixels of W.

Consequently, the modified condition (4) for the noisy pixel detection is

$$\frac{\widehat{D_1} - \widehat{D_{(1)}}}{m} > T, \quad \widehat{D_{(1)}} = min\{D_i : i = 1, \dots, v\} \tag{6}$$

As local image textural elements and minute details are taken into account, this decision-making process becomes more reliable and precise. The suggested design will be called Adaptive Switching Trimmed (AST).

The trimmed sums in the AST scheme must be calculated for each pixel in W in order to identify the minimum one. Although this technique has a high computing efficiency, as will be demonstrated later, it still necessitates a significant number of distance computations for each pixel in the processing window, in addition to requiring the determination of the lowest value. The AST scheme is summarized in Fig. 2.

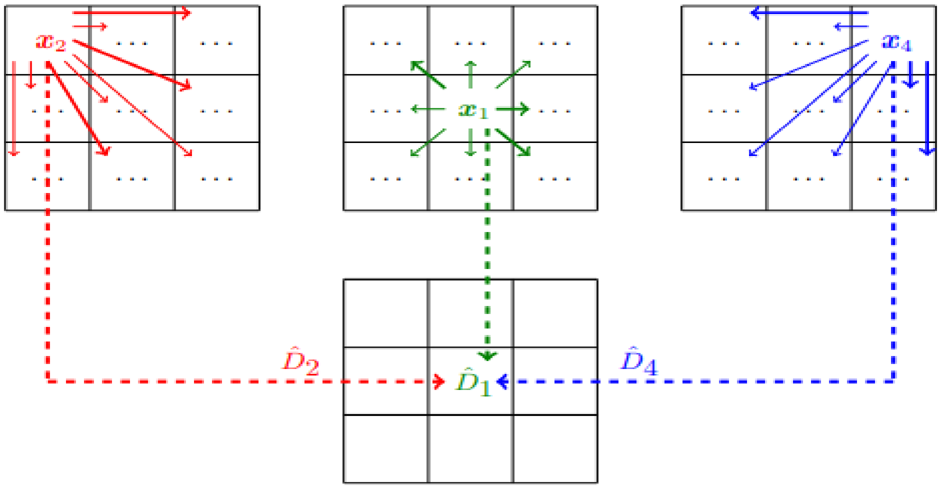

Fig.2 The AST design (a) requires the calculation of a trimmed sum of distances for every pixel of W to determine their minimum value, which is assigned to the central pixel.

The modelling of impulsive noise may be done in a variety of ways. The so-called "colour salt & pepper noise" is one of the most common contamination models. It assumes that a portion of the image pixels, designated by the symbol p, is damaged such that the RGB channels are given either the lowest or maximum value of the permitted dynamic range (0 or 255 assuming 8 bit channel representation). It is possible for the pixel affected by impulsive noise to become completely distorted, in which case all three channels would be replaced by extreme values, but it is also possible for one or two of the pixel's components to stay intact. Three channels are constantly influenced by the noise distortion, which can either be fully correlated or modelled using a known correlation of channel contamination.

The fact that only the extreme values of the damaged pixels should be repaired makes it easier to get rid of the salt and pepper noise. As a result, a more difficult and accurate noise model implies that each channel in a pixel that is impacted is changed to a random variable chosen at random from the uniform distribution.

Algorithm-1 describes the Overall Process of an algorithm and Algorithm-2 describes the Adaptive Switching Trimmed VMF Algorithm.

Algorithm-1: OVERALL ALGORITHM

---

a. Begin / Start

b. For each coloured image:

1. Validate if the image quality of the image is at the accepted level
2. If the image quality is at an acceptable level Go to step C
3. If the image quality is not at the accepted level, validate whether pre-processing is required or not
4. If pre-processing is not required then Go to Step 7
5. If pre-processing is required then apply the **Adaptive Switching Trimmed VMF Technique**

6. Apply Step 5 till the image reaches the accepted level
7. Apply the Noisy Pixel Detection algorithm on the image received
c. Stop

Algorithm-2: ADAPTIVE SWITCHING TRIMMED VMF ALGORITHM

---

a. Begin / Start
b. For each coloured image:
1. Determine the accepted Threshold ***T***
2. Identify the operating window '***W***'
3. Identify '***n***' samples
4. Determine the center pixel $\boldsymbol{x_1}$ at the position (u, v)
5. Identify '***m'*** pixels that are similar to x_1
6. Calculate the sum of dissimilarities $(\boldsymbol{D_i})$ measures between the identified center pixel ($\boldsymbol{x_1}$) and the samples from Window (***W***)
7. Sort the distances in ascending order
8. Calculate the trimmed sum of distances between the number of nearest pixels taken for calculation
9. If the calculated trimmed sum of distances is less than the standard sum of distances then Go to Step 6
10. If the calculated distance value of the Center pixel $(\boldsymbol{D_1})$ is greater than the other similar pixels then mark the pixel as corrupt
11. If the distance D_i is very high, then re-adjust the distance by subtracting D_1 from the calculated Distance D_i
12. Create a Map $M_{(u,v)}$ where 0 is recognized as a corrupted pixel while 1 is identified as a non-corrupted pixel
13. Calculate whether another level of filter application is required or not
11.1 Divide the calculated $(\boldsymbol{D_1})$ ***by 'm' pixels***
11.2 Check if the value is greater than the predefined threshold **(T)**
11.3 If yes, then apply filter
11.4 Add a pixel to Map M
14. Validate if AST is required or not. If yes, go to Step 15, else go to Step 19
15. Calculate the trimmed sum of distances to the identified pixel
16. Calculate the minimum trimmed sum
17. Go to step 11
18. Repeat from Step 2 for all the pixels
19. Apply Noise pixel algorithms for the identified Pixels in Map M
c. Stop

Experimental Results

This study compares the presented Adaptive Switching Trimmed Filtering Algorithm to the state-of-the-art vector median filters using three test statistics. The root mean square error (RMSE), which is the first, is defined as

$$RMSE(X,Y) = \sqrt{\frac{1}{MN}\sum_{i=1}^{M}\sum_{j=1}^{N}\left\|X_{i,j} - Y_{i,j}\right\|^2} \quad (7)$$

where X and Y represent the original and filtered images, respectively. A small RMSE value indicates that the error between the filtered and original images is tiny. Hence, modest RMSE values are acquired.

The second measure is the peak signal-to-noise ratio (PSNR) which is defined as

$$PSNR(X,Y) = 10\log_{10}\left(\frac{Max(X)^2}{MSE(X,Y)}\right) \quad (8)$$

where MSE (X, Y) is the filtered image's mean square error. A high PSNR is preferred since it demonstrates a stronger signal to noise restoration.

The third measure is the structural similarity index (SSIM) which is defined as

$$SSIM(X,Y) = \frac{(2\mu_x + \mu_y + c_1)(2C_{x,y} + c_2)}{(\mu_x^2 + \mu_y^2 + c_1)(\sigma_x^2 + \sigma_y^2 + c_2)} \quad (9)$$

where the image means are

$$\mu_x = \frac{1}{N}\sum_{i=1}^{N} X_i \quad (10)$$

$$\mu_y = \frac{1}{N}\sum_{i=1}^{N} Y_i \quad (11)$$

Where C(.,.) signifies the covariance between the original and filtered pictures and σ^2 denotes the variance.

The SSIM value combines perceptual factors like brightness and contrast to represent how similar the original and filtered images are to one another. An elevated SSIM value means that the original image was accurately restored.

Fig. 3 is used to analyze the Adaptive Switching Trimmed VMF Algorithm denoising method experimentally.

Fig. 3 Original Test Image

As demonstrated in Fig. 4, which shows noisy and filtered images with different noise probabilities, the last column—which corresponds to the Adaptive Switching Trimmed VMF approach—performs better than the others. Figures 5, 6, and 7 illustrate PSNR vs noise probability, RMSE versus noise probability, and SSIM versus noise probability for test image under an exemplary implementation of the disclosure. As can be shown, our Adaptive Switching Trimmed VMF technique performs better in terms of accuracy (low RMSE) than methods and the efficiency rises as the noise probability rises.

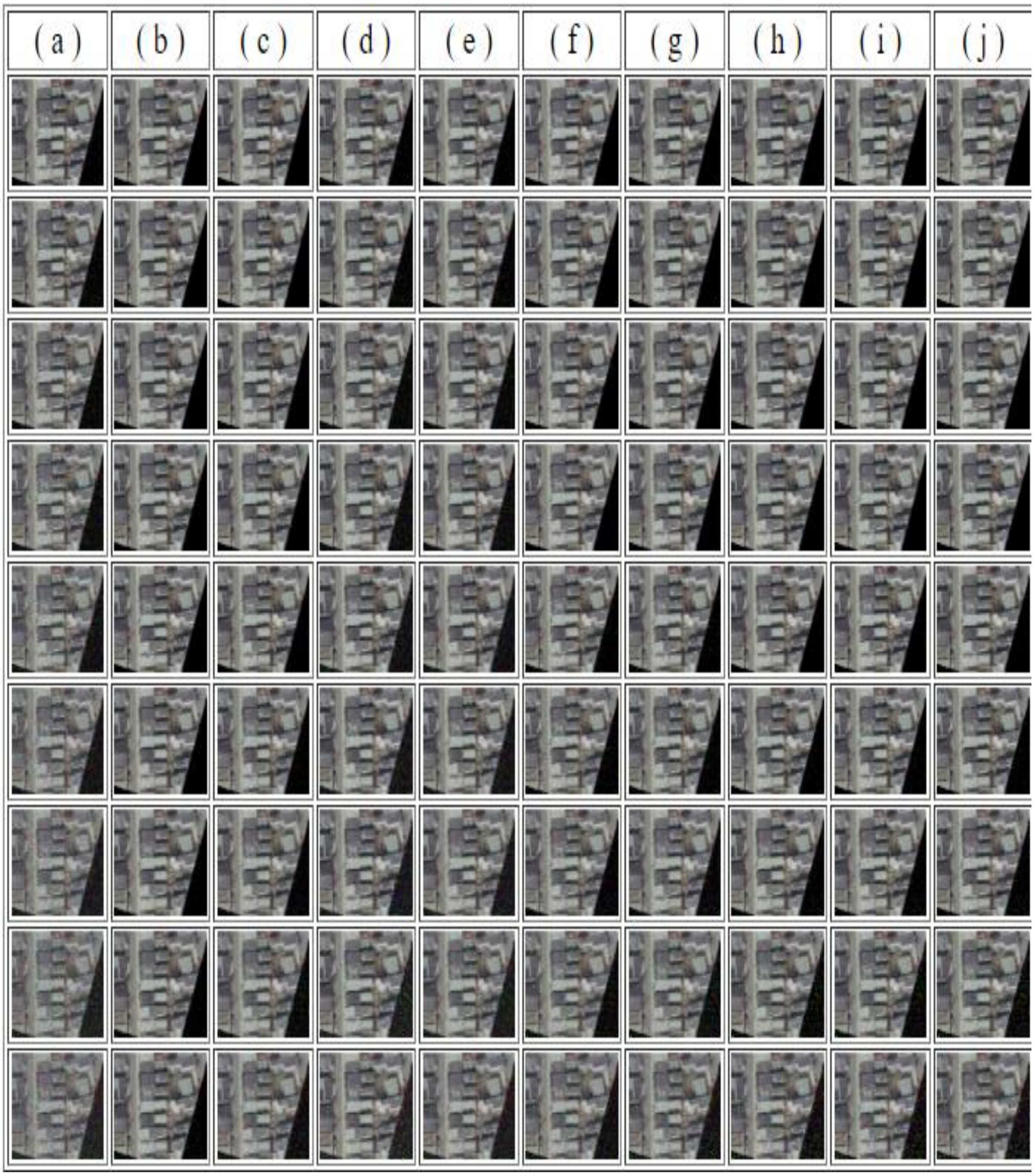

Fig. 4 Noise Reduction by various filters: Left to right: (a) Noisy image, (b) Median filter, (c) VMF, (d) BVDF, (e) DDF, (f) DVMF, (g) VMFDD, (h) ARWSF, (i) Alpha trim VMF, (j) ASTVMF. Top to bottom: Noise probability p = 0.1, 0.2, 0.3, 0.4, 0.5, 0.6, 0.7, 0.8, 0.9, in accordance with an illustrative embodiment of the disclosure.

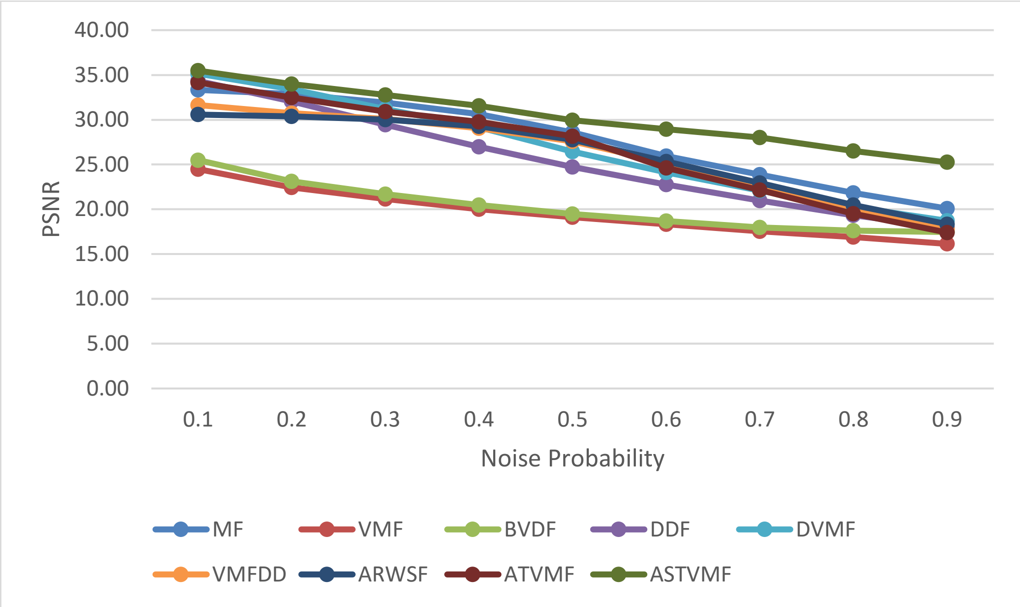

Fig. 5 The PSNR versus the Noise Probability for test image

Table 1. Shows the Psnr Values for the Images Shown in Fig.4

	MF	**VMF**	**BVDF**	**DDF**	**DVMF**	**VMFDD**	**ARWSF**	**ATVMF**	**ASTVMF**
0.1	33.33	24.49	25.49	34.33	35.14	31.64	30.57	34.15	35.48
0.2	32.86	22.45	23.13	32.06	33.42	30.73	30.38	32.48	33.98
0.3	31.90	21.14	21.71	29.46	31.19	30.09	30.02	30.91	32.76
0.4	30.61	20.03	20.49	26.99	29.16	29.06	29.25	29.77	31.55
0.5	28.58	19.11	19.47	24.74	26.44	27.59	27.76	28.16	29.96
0.6	25.94	18.32	18.69	22.77	24.11	25.21	25.33	24.61	28.94
0.7	23.88	17.56	17.98	20.99	22.08	22.76	22.96	22.15	28.00
0.8	21.82	16.91	17.62	19.34	20.26	20.04	20.46	19.52	26.52
0.9	20.09	16.15	17.46	17.98	18.72	17.78	18.35	17.41	25.25

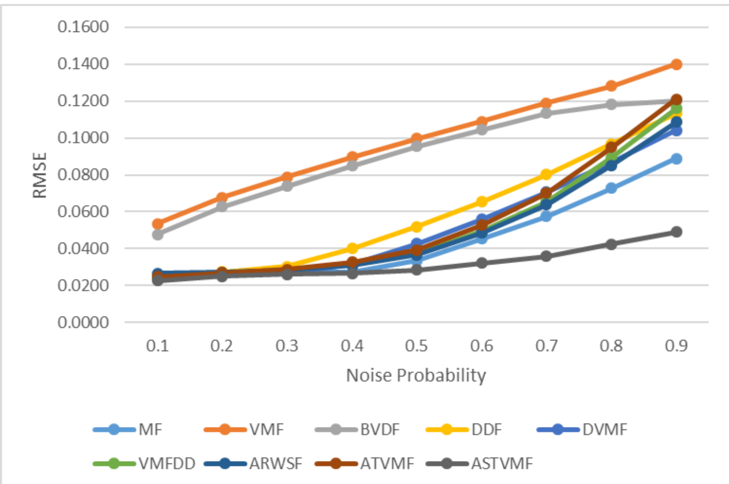

Fig. 6 The RMSE versus the Noise Probability for test image-1

Table 2. Shows the RMSE values for the images shown in Fig.4

	MF	**VMF**	**BVDF**	**DDF**	**DVMF**	**VMFDD**	**ARWSF**	**ATVMF**	**ASTVMF**
0.1	0.0237	0.0536	0.0477	0.0254	0.0240	0.0235	0.0266	0.0249	0.0228
0.2	0.0262	0.0678	0.0627	0.0274	0.0271	0.0261	0.0272	0.0269	0.0251
0.3	0.0273	0.0788	0.0738	0.0302	0.0268	0.0281	0.0283	0.0287	0.0260
0.4	0.0273	0.0896	0.0850	0.0402	0.0313	0.0317	0.0310	0.0328	0.0267
0.5	0.0335	0.0996	0.0955	0.0520	0.0428	0.0375	0.0368	0.0394	0.0285
0.6	0.0454	0.1090	0.1045	0.0653	0.0560	0.0493	0.0487	0.0528	0.0321
0.7	0.0575	0.1191	0.1135	0.0802	0.0707	0.0654	0.0639	0.0702	0.0358
0.8	0.0728	0.1282	0.1182	0.0969	0.0871	0.0894	0.0852	0.0949	0.0424
0.9	0.0890	0.1401	0.1203	0.1135	0.1041	0.1161	0.1086	0.1211	0.0491

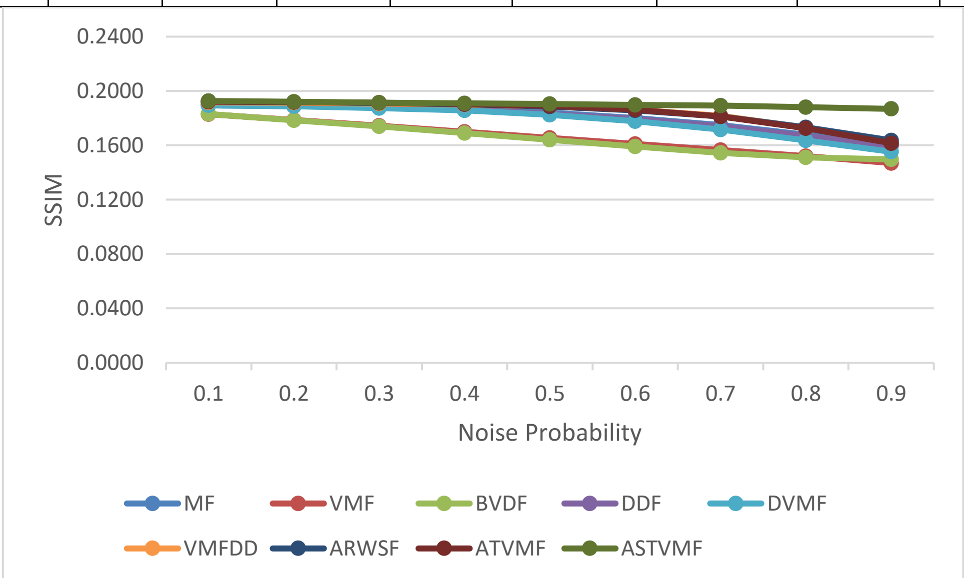

Fig. 7 The SSIM versus the Noise Probability for test image

Table 3. Shows the Ssim values for the Images Shown in Fig.4

	MF	VMF	BVDF	DDF	DVMF	VMFDD	ARWSF	ATVMF	ASTVMF
0.1	0.1894	0.1829	0.1830	0.1900	0.1894	0.1916	0.1925	0.1921	0.1926
0.2	0.1888	0.1786	0.1783	0.1892	0.1887	0.1913	0.1919	0.1919	0.1920
0.3	0.1878	0.1744	0.1740	0.1879	0.1874	0.1908	0.1912	0.1913	0.1914
0.4	0.1865	0.1699	0.1691	0.1861	0.1857	0.1900	0.1903	0.1905	0.1909
0.5	0.1840	0.1656	0.1640	0.1832	0.1824	0.1887	0.1886	0.1891	0.1904
0.6	0.1800	0.1611	0.1592	0.1794	0.1777	0.1861	0.1858	0.1861	0.1898
0.7	0.1750	0.1565	0.1545	0.1741	0.1716	0.1817	0.1813	0.1812	0.1893
0.8	0.1679	0.1520	0.1511	0.1669	0.1636	0.1731	0.1734	0.1724	0.1880
0.9	0.1604	0.1470	0.1497	0.1597	0.1553	0.1620	0.1637	0.1616	0.1868

Another method for demonstrating their superiority is through structural similarities. The Adaptive Switching Trimmed VMF strategy surpasses the VMF method at p= 0.2, but it becomes more effective at p= 0.9, achieving a 19% efficiency. It indicates that impulse noise reduction is improved by Adaptive Switching Trimmed VMF of just the valid pixels, or those pixels in the signal space that are said to hold significant information.

Conclusion

In this paper, a novel technique called adaptive switching trimmed VMF is presented for reducing impulse noise in satellite images. Traditional filtering approaches, most frequently the vector median filtering approach and its variations, apply a noise reduction algorithm to the center pixel of a well-designed window that iteratively slides through the entire image. To determine the smallest pixel in a Window, the trimmed sums in the AST scheme must be computed for each pixel in the Window. The accuracy of the Adaptive Switching Trimmed VMF approach is higher (low RMSE), and efficiency increases with increasing noise probability. At p= 0.2, this approach outperforms the VMF method, but at p= 0.9, it becomes even more successful, obtaining a 19% efficiency. It shows that Adaptive Switching Trimmed VMF of just the valid pixels, or those pixels in the signal space that are supposedly contain significant information, improves impulsive noise reduction.

References

1. SwathiLakshmanan, U. and Jeseena, A., An improved image denoising method based on Gradient Histogram Preservation.
2. Yogesh, V. and Yogendra, K., 2013. Removal of Salt and Pepper Noise from Satellite Images. *International Journal of Engineering Research & Technology (IJERT)*, *2*, pp.2051-2058.
3. Pitas, I. and Venetsanopoulos, A.N., 2013. *Nonlinear digital filters: principles and applications* (Vol. 84). Springer Science & Business Media.
4. Sicuranza, G., 2000. *Nonlinear image processing*. Elsevier.
5. Nodes, T. and Gallagher, N., 1982. Median filters: Some modifications and their properties. *IEEE Transactions on Acoustics, Speech, and Signal Processing*, *30*(5), pp.739-746.
6. Ng, P.E. and Ma, K.K., 2006. A switching median filter with boundary discriminative noise detection for extremely corrupted images. *IEEE Transactions on image processing*, *15*(6), pp.1506-1516.
7. Sun, T. and Neuvo, Y., 1994. Detail-preserving median based filters in image processing. *Pattern recognition letters*, *15*(4), pp.341-347.
8. Florencio, D.A. and Schafer, R.W., 1994, September. Decision-based median filter using local signal statistics. In *Visual Communications and Image Processing'94* (Vol. 2308, pp. 268-275). SPIE.
9. Chen, T., Ma, K.K. and Chen, L.H., 1999. Tri-state median filter for image denoising. *IEEE Transactions on Image processing*, *8*(12), pp.1834-1838.
10. Wang, Z. and Zhang, D., 1999. Progressive switching median filter for the removal of impulse noise from highly corrupted images. *IEEE Transactions on Circuits and Systems II: Analog and Digital Signal Processing*, *46*(1), pp.78-80.
11. Zhang, S. and Karim, M.A., 2002. A new impulse detector for switching median filters. *IEEE Signal processing letters*, *9*(11), pp.360-363.
12. Eng, H.L. and Ma, K.K., 2001. Noise adaptive soft-switching median filter. *IEEE Transactions on image processing*, *10*(2), pp.242-251.
13. Xu, Q., Zhang, Q., Hu, D. and Liu, J., 2018. Removal of salt and pepper noise in corrupted image based on multilevel weighted graphs and IGOWA operator. *Mathematical Problems in Engineering*, *2018*.
14. Kumar, N.R. and Kumar, J.U., 2015. A spatial mean and median filter for noise removal in digital images. *International Journal of Advanced Research in Electrical, Electronics and Instrumentation Engineering*, *4*(1), pp.246-253.
15. J. Astola, P. Haavisto and Y. Neuvo, "Vector median filters," in Proceedings of the IEEE, vol. 78, no. 4, pp. 678-689, April 1990, doi: 10.1109/5.54807.
16. Khryashchev, V., Kuykin, D. and Studenova, A., 2011. Vector median filter with directional detector for color image denoising. In *Proc. of the World Congress on Engineering* (Vol. 2, pp. 1-6).
17. Plataniotis, K.N., Androutsos, D. and Venetsanopoulos, A.N., 1997, May. Vector directional filters: An overview. In *CCECE'97. Canadian Conference on Electrical and*

Computer Engineering. Engineering Innovation: Voyage of Discovery. Conference Proceedings (Vol. 1, pp. 106-109). IEEE.

18. Chanu, R. and Singh, K.M., 2016. Vector median filters—A survey. *International Journal of Computer Science and Network Security*, *16*(12), pp.66-84.
19. Trahanias, P.E. and Venetsanopoulos, A.N., 1993. Vector directional filters-a new class of multichannel image processing filters. *IEEE Transactions on Image Processing*, *2*(4), pp.528-534.
20. Lukac, R., 2004. Adaptive color image filtering based on center-weighted vector directional filters. *Multidimensional Systems and Signal Processing*, *15*(2), pp.169-196.
21. Smolka, B., Malik, K. and Malik, D., 2015. Adaptive rank weighted switching filter for impulsive noise removal in color images. *Journal of Real-Time Image Processing*, *10*(2), pp.289-311.
22. Lukac, R., Smolka, B. and Plataniotis, K.N., 2007. Sharpening vector median filters. *Signal Processing*, *87*(9), pp.2085-2099.
23. Smolka, B., 2014, August. Robustified vector median filter. In *2014 9th International Conference on Computer Science & Education* (pp. 362-367). IEEE.
24. Smolka, B., Andrzejczak, A., Nabialkowski, P. and Nelip, A., 2014, July. Thresholded median filter for the impulsive noise removal in digital images. In *IISA 2014, The 5th International Conference on Information, Intelligence, Systems and Applications* (pp. 355-360). IEEE.